Crystallization, morphology, structure and thermal behaviour of nylon-6/rubber blends

E. Martuscelli, F. Riva, C. Sellitti and C. Silvestre
Istituto di Ricerche su Tecnologia dei Polimeri e Reologia del C.N.R. Via Toiano 6, 80072 Arco Felice (Napoli) Italy
(Received 23 March 1984)

An experimental study was carried out in order to investigate the morphological, kinetic, structural and thermodynamic properties of nylon-6/rubber (namely ethylene–propylene copolymer (EPM) and ethylene–propylene copolymer functionalized by inserting along its backbone succinic anhydride groups (EPM-g-SA)) blends. The morphology and the overall kinetics of crystallization of the blends strongly depend on the type of copolymer added to nylon and on the blend composition. The EPM-g-SA acts as a nucleating agent for the Ny spherulites and at the same time causes a drastic depression of the overall kinetic rate constant. This decrease is related to the increase of the melt viscosity observed in Ny/EPM-g-SA blends. The crystalline lamella thickness of the Ny phase in the blends is lower than that of pure Ny crystallized at the same T_c suggesting that the presence in the melt of an elastomeric phase disturbs the growth of the Ny crystals. The rubber does not influence the thermal behaviour of the nylon. The results found lead to the conclusion that in the melt nylon-6 is incompatible with both EPM and EPM-g-SA copolymers.

(Keywords: nylon-6; ethylene–propylene copolymers; blend crystallization; morphology; thermal behaviour)

INTRODUCTION

The morphology–property relationships of nylon-6/rubber blends obtained by melt mixing were studied and the results have been published previously[1-3]. An ethylene–propylene random copolymer (EPM) and an EPM chemically functionalized, by inserting along its backbone a certain number of succinic anhydride groups (EPM-g-SA), were used as rubbery components[1-3]. It was found that binary Ny 6/EPM-g-SA and ternary Ny 6/EPM-g-SA/EPM blends show a very fine distribution of the rubber in the Ny 6 matrix and, consequently, noticeably better impact properties with respect to those of nylon-6 and binary Ny 6/EPM blends. Such results were interpreted by assuming that during melt mixing a graft copolymer, able to act as interfacial and emulsifying agent, is formed between the functionalized EPM-g-SA rubber and nylon-6. This graft copolymer [(EPM-g-SA)-g-Ny 6)] is obtained by means of a heat induced condensation between the EPM-g-SA carboxylic groups of EPM-g-SA molecules and the $-NH_2$ terminals of polyamide molecules[1,3].

In the present paper we report the results of an investigation concerning the influence of composition, chemical nature of rubber components and crystallization conditions on:

(a) the primary nucleation, overall crystallization and thermal behaviour of Ny 6 from its blends with EPM and EPM-g-SA;

(b) the overall morphology of the blends (dimensions of nylon 6 spherulites and of the rubber domains) and the super-reticular structure (long spacing and crystalline lamella thickness) as well as the polymorphism phenomenon.

EXPERIMENTAL

Materials

In the present paper the following materials were used: polyamide-6 (Ny 6) $\bar{M}_n = 230\,000$ supplied by SNIA and as rubbery components an amorphous, Dutral CO/O54, ethylene–propylene copolymer (EPM) having 60% by moles of C_2, kindly supplied by Montedison, and a

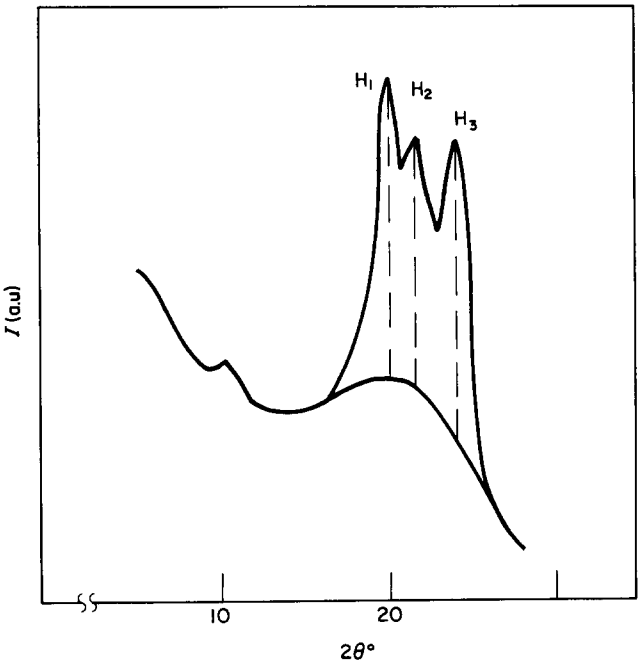

Figure 1 X-ray diffraction pattern of nylon-6 (CuK_α Ni-filtered radiation)

0032-3861/85/020270-13$03.00

modified EPM bearing, along its backbone, 2.7% by weight of succinic acid groups (EPM-g-SA), prepared in the synthesis laboratory of our Institute[1-3].

Blend preparation

The binary and ternary blends were obtained by melt mixing the components in a Brabender-like apparatus (Rheocord of Haak Inc.) at 260°C and 32 rpm for 20 min. Thin sheets of the samples were prepared by compression moulding in a common heated press. Then they were conditioned in order to absorb the same amount (about 3%) of water that they would have acquired under equilibrium conditions in an environment with 50% of relative humidity. More details on the blend preparation and on the process of conditioning are reported in previous papers[1-3].

Wide angle X-ray scattering (WAXS)

WAXS patterns (CuKα, Ni-filtered radiation) were collected by a flat camera (sample-film distance $D=75$ mm) and analysed by a Nicolet AD-1 microcomputerized densitometer (scanning plane XY, resolving power up to 10 μ). From densitometer traces the γ form index, I_γ, was calculated, for nylon 6. The following Kyotani[4] equation was used:

$$I_\gamma = \frac{H_2}{H_1 + H_2 + H_3}$$

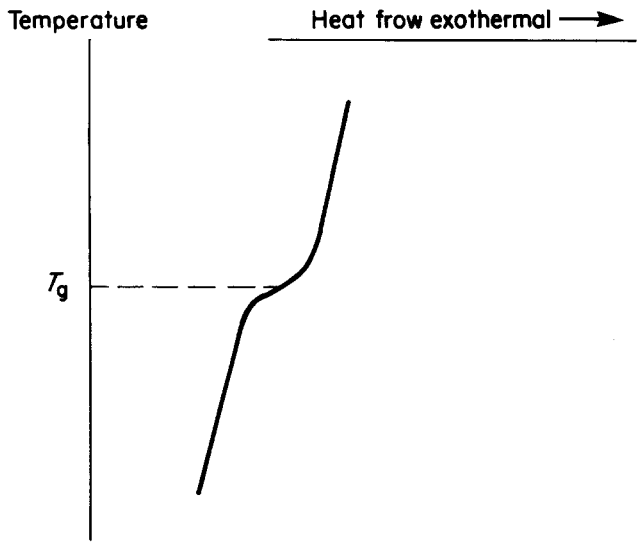

Figure 2 Method used for the determination of the glass transition temperature

where H_1 and H_3 are the heights of the (200) and (002)+(202) crystalline reflections of α form and H_2 is the height of the (001) crystalline reflection of Ny 6 γ form, in the 2θ region between 20° and 25° (*Figure 1*).

Small angle X-ray scattering (SAXS)

SAXS patterns (CJKα, Ni-filt. radiation) were collected by a Rigaku Denki photographic camera using a collimation pinhole system and a sample-film distance of 330 mm. From such patterns the long spacing, L, was derived by applying the Bragg law.

Morphology investigation

The overall morphology of the blends was investigated by optical and scanning electron microscopy. Optical

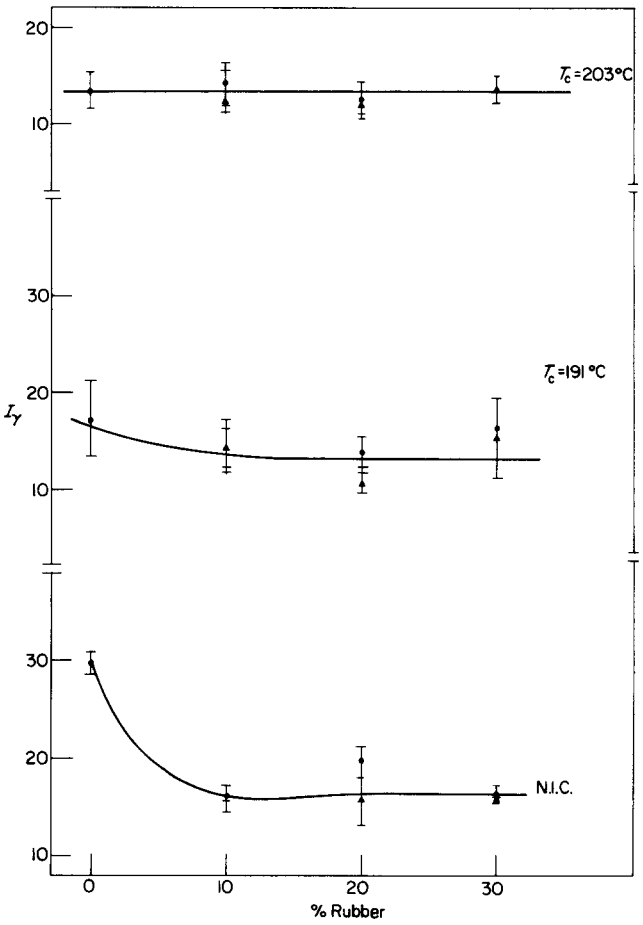

Figure 3 δ form index (I_δ) as function of rubber content for I.C. and N.I.C. samples. (●) Ny/EPM; (▲) Ny/EPM-g-SA

Table 1 Crystallinity index, x_c, for nylon rubber blends crystallized from the melt (x_c by d.s.c.)

Rubbery component	(%)	N.I.C.		I.C. T_c = 464 K		I.C. T_c = 476 K	
		x_c (blend)	x_c (Ny 6)	x_c (blend)	x_c (Ny 6)	x_c (blend)	x_c (Ny 6)
EPM	0	0.26	0.26	0.29	0.29	0.29	0.29
	10	0.23	0.26	0.25	0.28	0.23	0.26
	20	0.20	0.25	0.22	0.28	0.22	0.28
	30	0.19	0.27	0.20	0.29	0.21	0.30
EPM-g-SA	10	0.24	0.27	0.26	0.29	0.25	0.28
	20	0.18	0.23	0.22	0.28	0.23	0.29
	30	0.16	0.23	0.19	0.27	0.17	0.24

The error on the crystallinity index is ± 0.03
N.I.C. = Non isothermally crystallized
I.C. = Isothermally crystallized

Table 2 Super-reticular parameters for nylon 6 isothermally crystallized from its blends with EPM rubbers

% Ny 6	EPM	Long period L (Å)		Crystalline lamella thickness L_C (Å)	
		T_C = 464 K	T_C = 476 K	T_C = 464 K	T_C = 476 K
100	0	128	134	37	39
90	10	113	123	32	32
80	20	111	125	31	35

The error on L and L_C values is about ± 7%

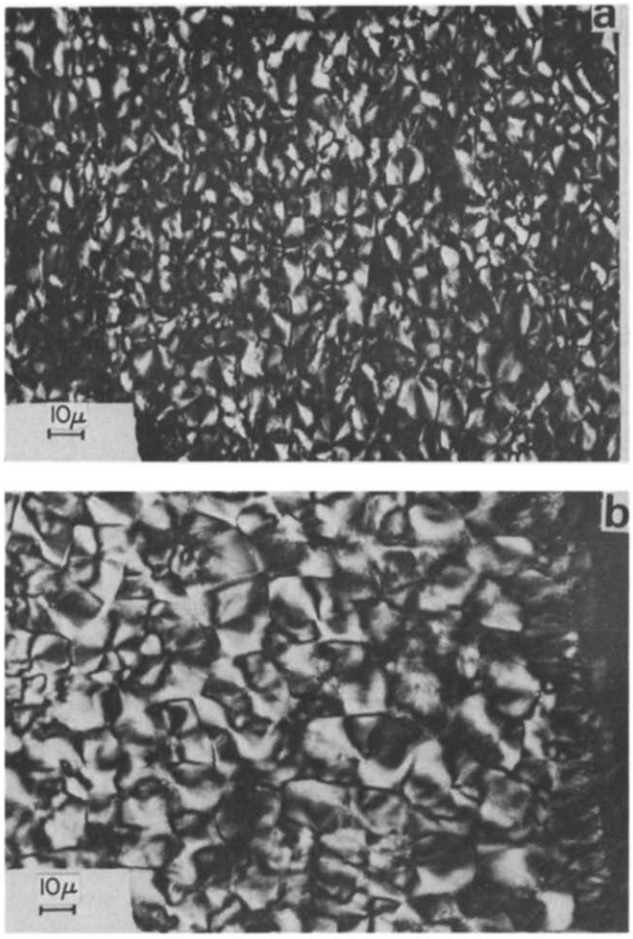

Figure 4 Photomicrographs of pure nylon (a) non-isothermally crystallized sample optical photomicrographs with crossed polars; (b) isothermally crystallized sample, T_c=476 K

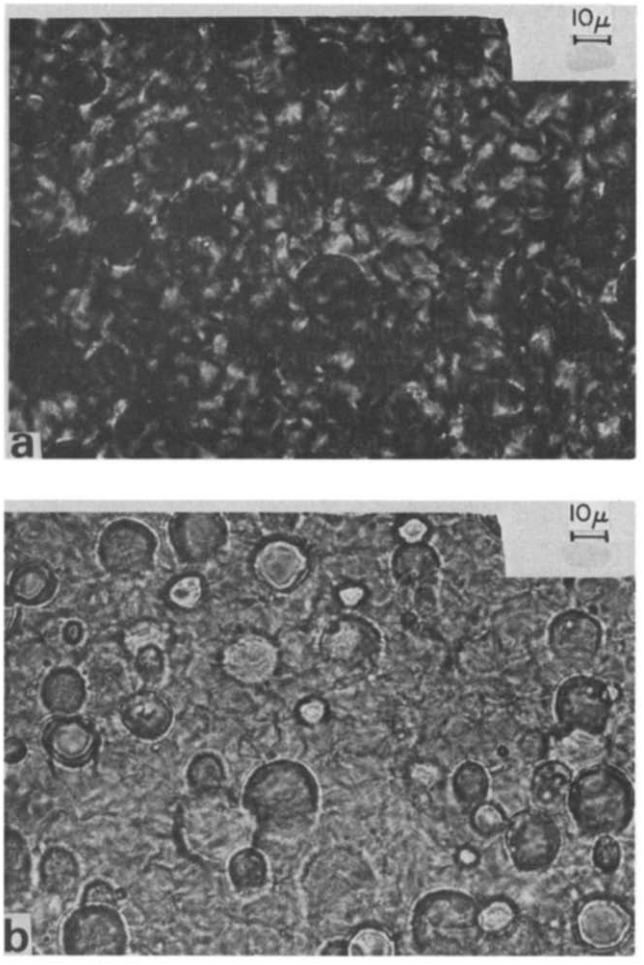

Figure 5 Photomicrographs of Ny/EPM 90/10 blend, samples isothermally crystallized (a) crossed polars, (b) parallel polars

micrographs were taken by using a Leitz Ultraphot microscope on sections of the samples isothermally crystallized in the d.s.c. aluminium pan (I.C. samples) and on samples cooled to room temperature after compression moulding (N.I.C. samples).* Scanning electron microscopy was carried out by using a SEM Philips 501. Before electron microscopy studies, samples of binary and ternary blends were faced in a ultramicrotome LKB (Ultramicrotome III) at room temperature and the resulting smooth surfaces were coated with gold/palladium.

Calorimetric measurements

The overall kinetics of crystallization and the thermal properties of the homopolymer and blends were analysed by using differential scanning calorimetry.

The isothermal crystallization process was studied by using a Perkin Elmer DSC-2 with the following procedure: the samples (about 7 mg) were heated up to 20° above the melting temperature of the Ny 6 and kept at this temperature for 15 min. Thereafter the samples were rapidly cooled to the desired crystallization temperature, T_c, and the heat dH/dt evolved during the isothermal crystallization was recorded as a function of time. The weight fraction X_t of the material crystallized at time t was calculated from the ratio between the heat generated at time t and the total heat corresponding to the completion of the crystallization. The observed melting temperature, T'_m, and the apparent enthalpies of melting, ΔH^*, of the isothermally crystallized samples were obtained from the maxima and the area, respectively, of the melting peaks, obtained heating the samples directly from T_c to the melting point at a scanning rate of 20°C min^{-1}.

The crystallinity index of the Ny phase x_c(Ny) and of the overall blend x_x(blend) was calculated by means of the following relations:

$$x_c(\text{Ny}) = \frac{\Delta H^*(\text{Ny})}{\Delta H^\circ(\text{Ny})} \qquad x_c(\text{blend}) = \frac{\Delta H^*(\text{blend})}{\Delta H^\circ(\text{Ny})}$$

*N.I.C. = Non isothermally crystallized

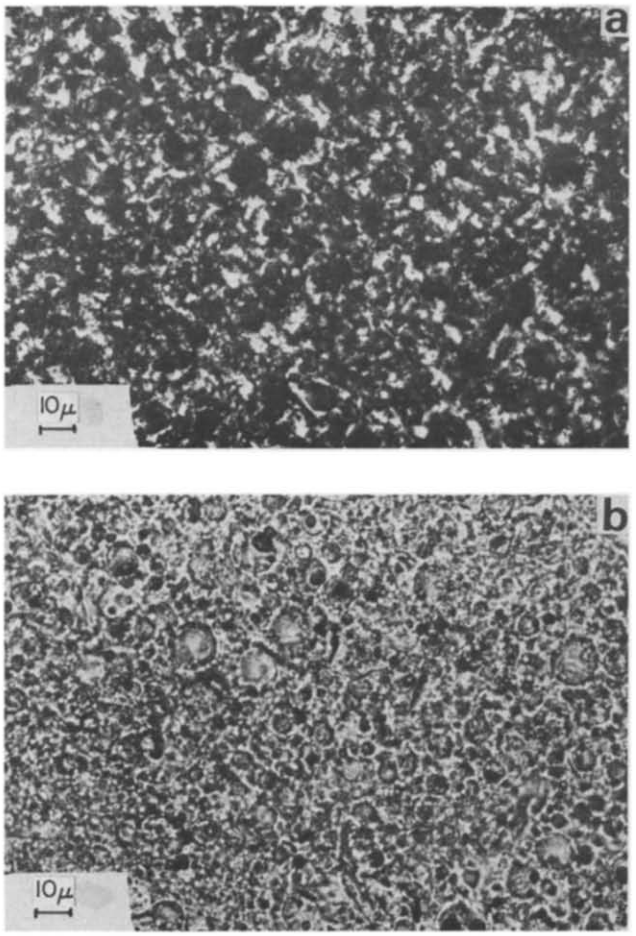

Figure 6 Optical micrographs of Ny/EPM 80/20 isothermally crystallized at T_c=476 K (a) crossed polars, (b) parallel polars

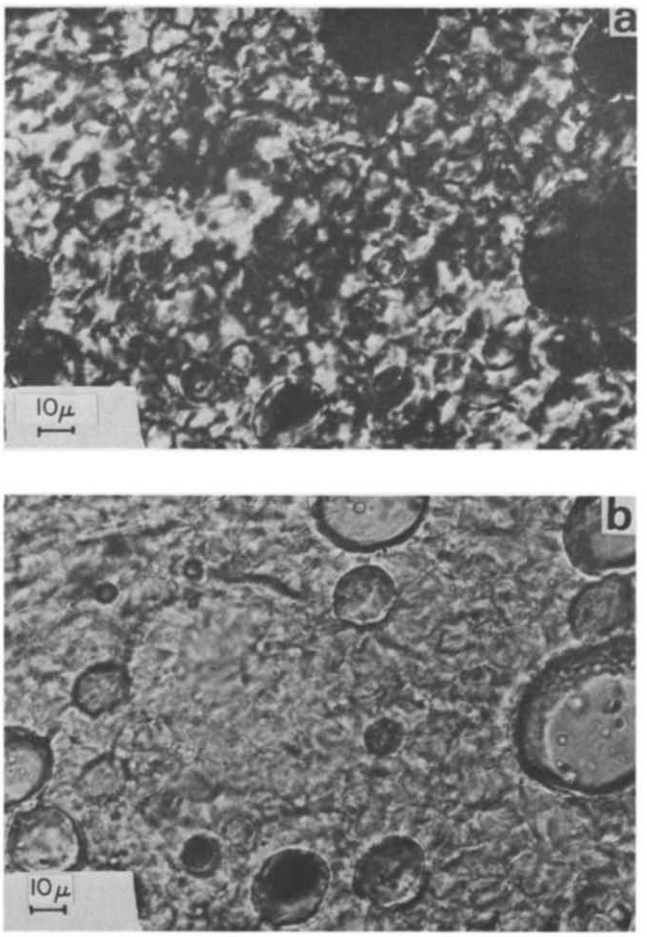

Figure 7 Optical micrographs of Ny/EPM 70/30 isothermally crystallized at T_c=476 K (a) crossed polars, (b) parallel polars

where ΔH^*(Ny) is the apparent enthalpy of melting per gram of Ny in the blend; $\Delta H°$(Ny) is the heat of fusion per gram of 100% crystalline Ny (from literature data ΔH(Ny)=49 cal g^{-1} (5) and ΔH^*(blend) is the apparent enthalpy of melting per gram of blend.

The glass transition temperatures were obtained by using a Mettler 3000 DSC with the following procedure: the samples (about 20 mg) were heated from −100°C up to 120°C at 20°C min^{-1} and the heat dH/dt, evolved during this scanning process was recorded as a function of temperature.

The T_g of the sample was taken as the temperature corresponding to 50% of the transition, as indicated in *Figure 2*.

RESULTS AND DISCUSSION

Crystallinity index measurements

The d.s.c. crystallinity index of the blends, x_c(blends), and that of Ny 6 phase x_c(Ny 6) are reported in *Table 1*. As expected the x_c(blends) and x_c(Ny 6) of N.I.C. samples are lower than those of the samples isothermally crystallized. For the same crystallization conditions the values of x_c(blend) decrease with the increase of rubber, whereas the x_c(Ny 6) is almost independent of composition.

Structural analysis

It is well known that the Ny 6 may crystallize in two different crystalline forms, namely α and γ [6]. The nucleation, growth and the relative amount of such crystalline forms depend on the crystallization conditions. It has been found that the Ny 6 crystallizes from the melt simultaneously in both α and γ forms. The γ form grows predominantly at lower T_c (below 130°C) and the amount of the α form increases with increasing T_c. The dependence of γ form index, I_γ, for the I.C. and N.I.C. samples, on the rubber content is reported in *Figure 3*. As shown, I_γ is almost independent of the rubber content in the case of Ny/EPM and Ny/EPM-g-SA blends isothermally crystallized at higher temperatures. By contrast a large drop in I_γ is observed when the blends are not isothermally crystallized.

Super-reticular analysis by SAXS

In *Table 2* the long period, $\underline{L}$, is reported as a function of T_c and composition for Ny/EPM blends. In the case of Ny/EPM-g-SA and Ny/EPM/EPM-g-SA blends the SAXS patterns show only a diffuse scattering: according to Hosemann's theory [7] this may generally indicate that the polydispersity of the overall Ny/rubber system is greater than the packing density.†

In *Table 2* are reported also the values of the crystalline lamella thickness, L, of the polyamide phase. The L_c values were calculated from the $\underline{L}$ values by using, as a first approximation, the relation:

† According to the Hosemann theory, a continuous scattering arises when the particle dimension polydispersity, g_y (defined as $g_y = \sqrt{\bar{y}^2 - \bar{y}^2}/\bar{y}^2$, $\bar{y}$ being the average radius of the particles), is larger than the packing density, ε [3]

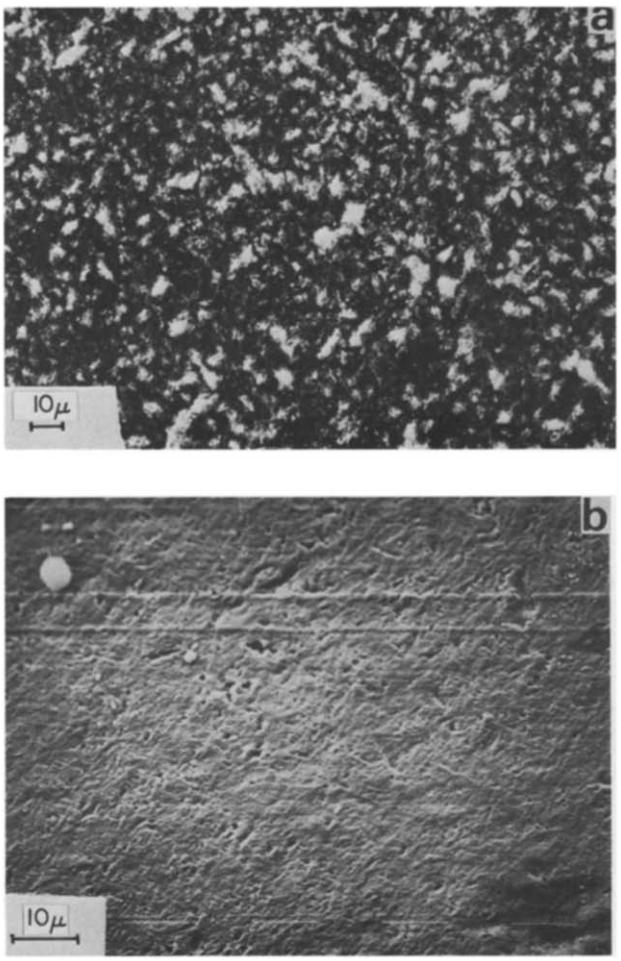

Figure 8 Photomicrographs of Ny/EPM-g-SA 90/10 blends isothermally crystallized at T_c=476 K (a) optical photomicrograph crossed polars, (b) electron photomicrograph

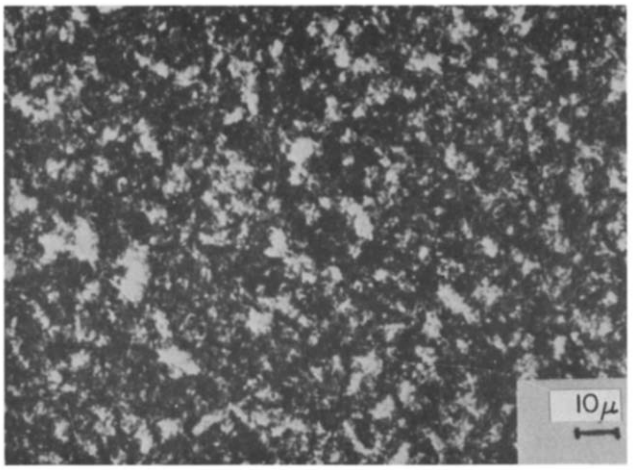

Figure 9 Optical photomicrographs with crossed polars of Ny/EPM-g-SA 80/20 blend isothermally crystallized at T_c=476 K

$$L_c = Lx_c(\text{Nylon}) \quad (1)$$

As shown, L increases with the increase of T_c and, for a given T_c, decreases with increasing rubber content.

From the values of L_c it emerges that when Ny crystallizes from its blends in the presence of EPM rubber, lamellar crystals are formed with slightly lower thickness

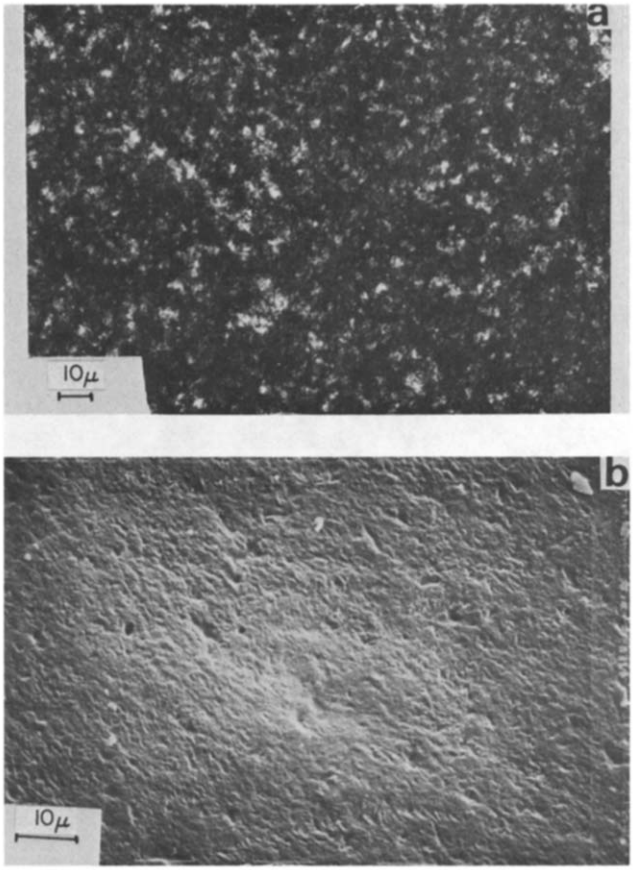

Figure 10 Photomicrographs of the 70/30 Ny/EPM-g-SA blend (a) optical micrograph with crossed polars, (b) electron micrograph

(measured along a direction that is almost coincident with the chain axis).

Morphology

Optical photomicrographs of the isothermal (I.C.) and non-isothermal (N.I.C.) crystallized Ny 6 samples are shown in *Figure 4*. The isothermally crystallized Ny samples present a double morphology: spherulitic and row. The row-like structure is present in the material crystallized in contact with the walls of the aluminium pan of the d.s.c. This row-like morphology results from a higher concentration of aligned nuclei on the sample-pan contact surface. Such nuclei can either pre-exist, i.e. they are not completely destroyed during the melting and migrate toward the surface before the crystallization starts and/or are formed during the isothermal crystallization process; it is in fact well known that cavities or rough surfaces are able to catalyse the formation of crystallization nuclei.

The presence of a row-like structure is, moreover, usually observed when a polymeric material crystallizes non isothermally on cold surfaces. In this case such a phenomenon is to be attributed to the effect of a thermal gradient. This last eventuality is not consistent with the isothermal crystallization condition used by us.

On adding EPM and/or EPM-g-SA to the Ny it is observed, for all the samples, that the row-like morphology disappears. This result leads to the hypothesis that the rubber hampers the migration of the nuclei to the surfaces and/or that the nuclei are de-

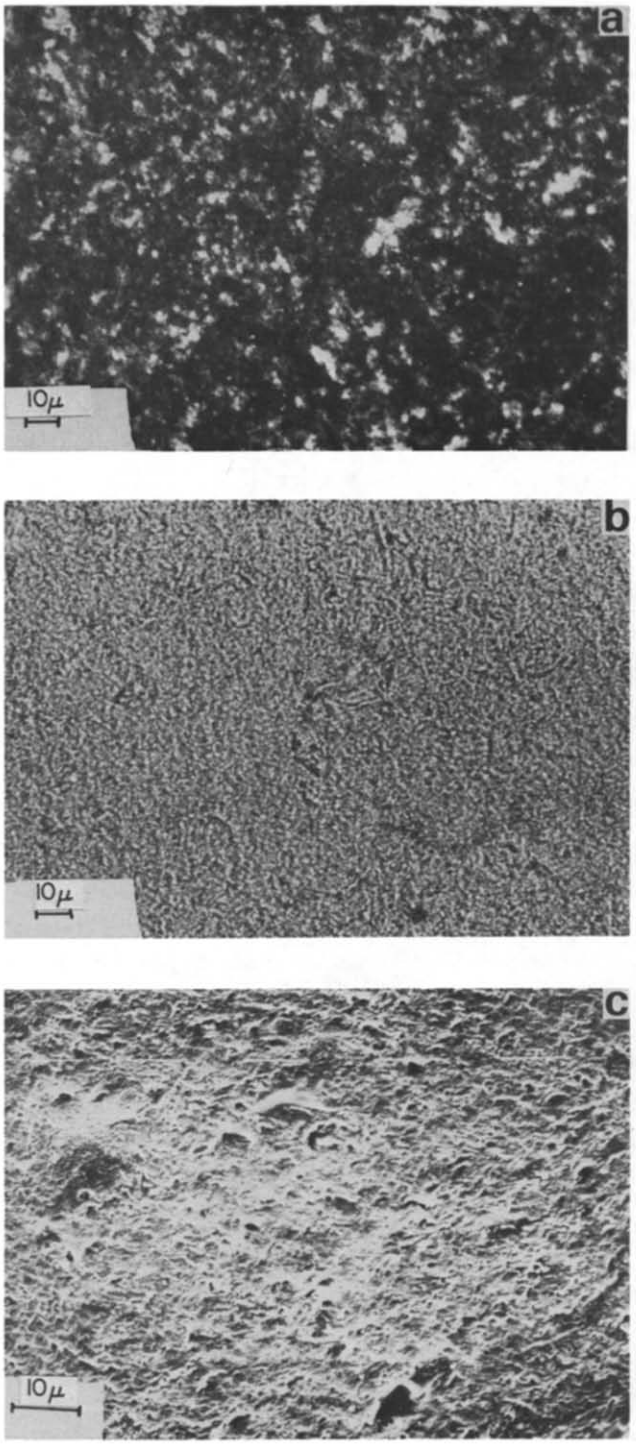

Figure 11 Photomicrographs of the 80/15/5 Ny/EPM/EPM-g-SA blend isothermally crystallized (a) optical micrograph with crossed polar, (b) optical micrograph with parallel polar, (c) electron micrograph

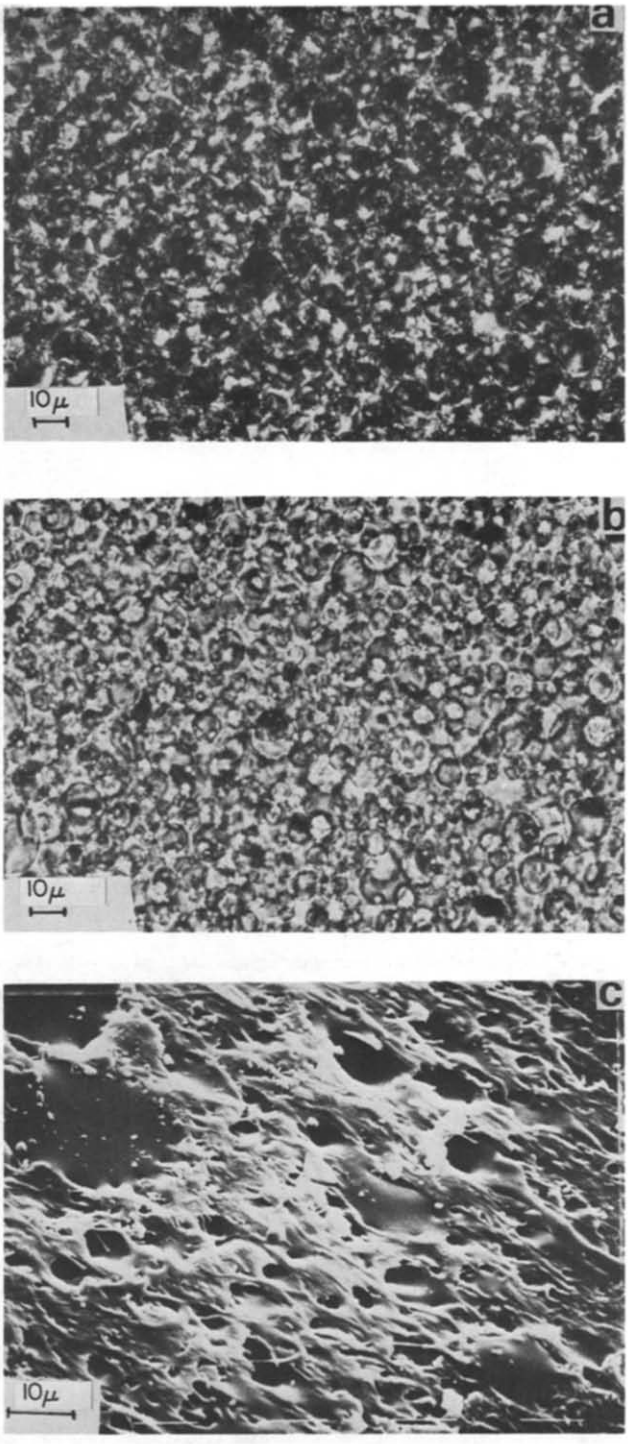

Figure 12 Photomicrographs of the 80/10/10 Ny/EPM/EPM-g-SA blend (a) optical micrograph with crossed polars, (b) optical micrograph with parallel polar, (c) electron micrograph

activated after the addition of the rubber, probably because they are incorporated into particles of the disperse phase. The overall morphology of the blends is therefore strongly dependent on the type of added copolymer and on the composition.

Ny/EPM blends. Photomicrographs of the Ny/EPM samples are reported in *Figures 5–7*. The distribution of the dimensions of the rubber domains in the case of 90/10 sample is very broad. The diameter of the particles of the disperse phase ranges from about 5 μm to 30 μm (see *Figure 5*).

For blends containing higher rubber percentages the distribution of the EPM particle dimensions is narrower: the average dimensions are about 10 μ and 50 μ for 80/20 and 70/30 Ny/EPM blends respectively (see *Figures 6* and *7*). The fact that for the 70/30 blends the rubber domains have larger dimensions indicates that coalescence phenomena may occur during the mixing in the melt and/or that the mixing procedure used for such blends does not produce a good dispersion of the rubber phase in the Ny matrix.

The morphological observations reported above seem to indicate that under the mixing conditions used in

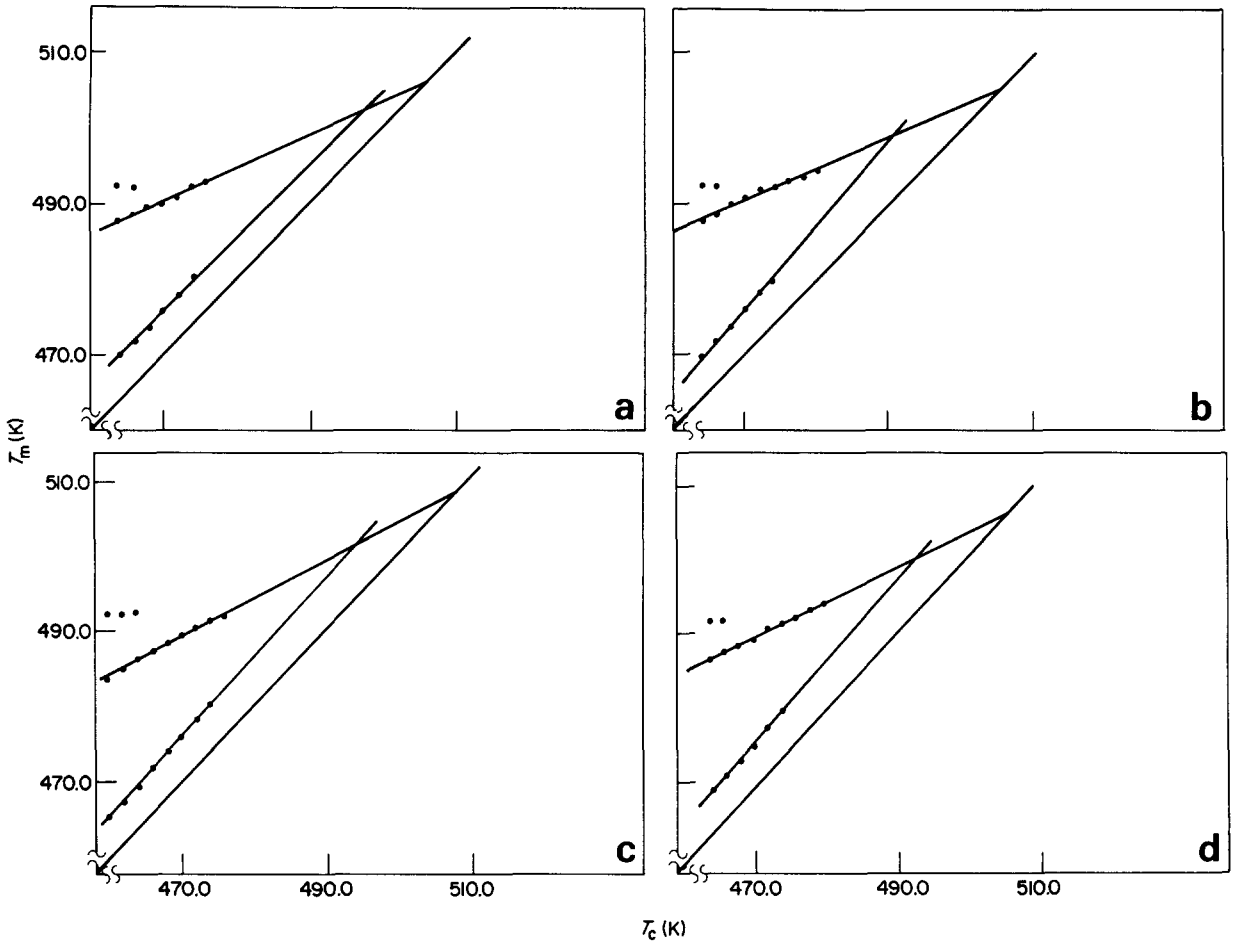

Figure 13 Observed melting temperatures, T_m, as function of crystallization temperature for (a) pure nylon; (b) 80/20 Ny/EPM blend, (c) 80/20 Ny/EPM-g-SA blend and (d) 80/10/10 Ny/EPM/EPM-g-SA blend

Ny/EPM blends there exists an optimal concentration of EPM (around 20% rubber) that leads to a material with a narrower size distribution of the disperse phase. The addition of EPM to Ny does not modify the dimensions and the structure of the Ny spherulites.

It is interesting to note that the dimensions of the EPM domains are close to or even larger than those of Ny spherulites. An opposite trend was observed in the case of isothermally crystallized iPP/rubber blends studied by Martuscelli and others[8,9]. In the latter case the rubber domain dimensions are smaller than those of iPP spherulites and depending on their rate of diffusion and on the growth rate of spherulites, they can be enclosed in intraspherulitic regions deeply altering the structure of spherulites.

Ny/EPMigiSA blends. Optical and electron micrographs of Ny/EPM-g-SA blends, isothermally crystallized at 476 K, for different composition, are shown in *Figures 8–10*. It is interesting to observe that the addition of EPM-g-SA causes a drastic reduction in the Ny spherulite dimensions. Contrary to what is observed in the case of Ny/EPM blends, no dispersed phase can be distinguished on the microtomed sections of Ny/EPM-g-SA blends. This indicates that the EPM-g-SA component is very finely dispersed in the Ny matrix giving rise to a finer morphology.

Ny/EPM/EPM-g-SA blends. Micrographs of the 80/10/10 and 80/15/5 Ny/EPM/EPM-g-SA blends are shown in *Figures 11* and *12*. It is possible to observe the influence that the composition has on the morphology of the system. In fact for the blend containing only 5% of the functionalized rubber, the dispersed domains are of irregular shape and of large dimensions. By contrast the blends with the same amount of EPM and EPM-g-SA present a more homogeneous structure, very similar to that of the Ny/EPM-g-SA 80/20 blends. Such results seem to suggest that the modified copolymer (EPM-g-SA) is able to act as a true compatibilizer and emulsifying agent only when a comparable amount of EPM rubber is contained in the mixture.

Table 3

Sample		T_m (K)
Ny	100%	506
Ny/EPM	90/10	507
Ny/EPM	80/20	506
Ny/EPM	70/30	506
Ny/EPM-g-SA	90/10	510
Ny/EPM-g-SA	80/20	508
Ny/EPM-g-SA	70/30	506
Ny/EPM-g-SA	80/5/15	507
Ny/EPM/EPM-g-SA	80/10/10	506

The error on the T_m values is ± 2 K

Thermal behaviour

Melting temperatures. It is extensively reported in the literature that the d.s.c. thermograms of isothermally crystallized Ny 6 present three peaks of fusion[10–14]. The peak at higher temperature is supposed to correspond to

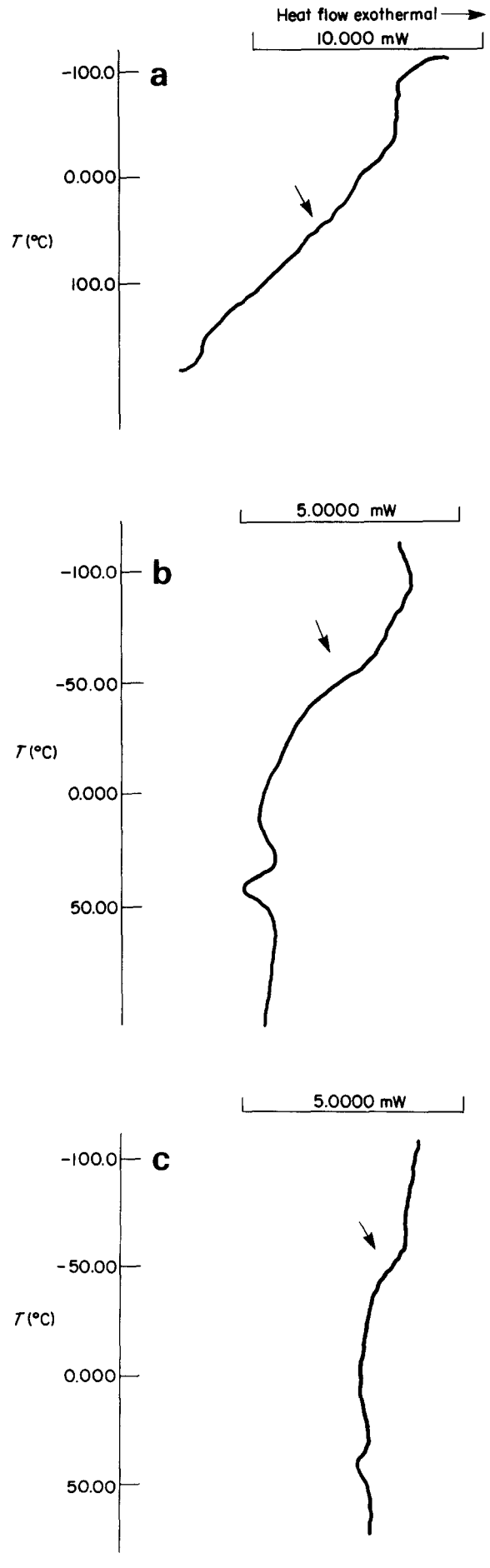

Figure 14 D.s.c. thermograms of (a) Ny, (b) EPM and (c) EPM-g-SA samples. Arrows indicate the region of glass transition

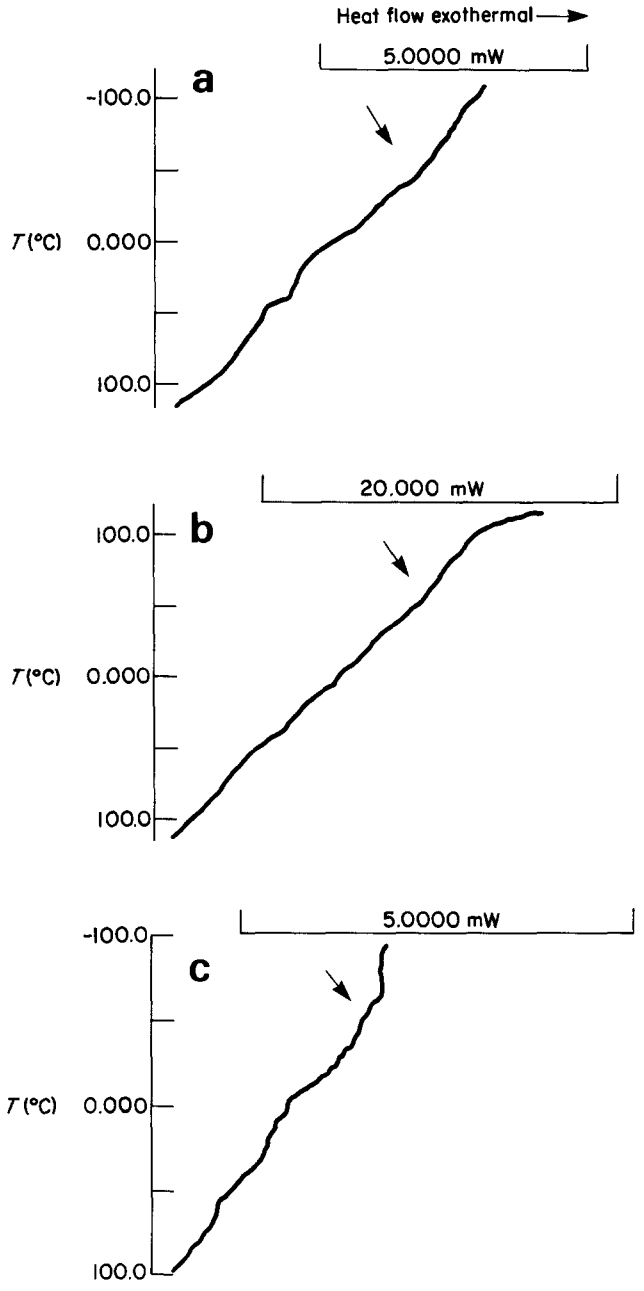

Figure 15 D.s.c. thermograms of (a) 80/20 Ny/EPM, (b) 80/20 Ny/EPM-g-SA and (c) 80/10/10 Ny/EPM/EPM-g-SA blends. Arrows indicate the region of glass transition

the fusion of Ny crystallized in the γ form, and that at lower temperature to the fusion of bundle-like chain crystals. Finally the peak at intermediate temperature corresponds to the melting of the α form of Ny 6. In agreement with the literature of the thermograms of Ny 6 studied in this paper present multiple fusion peaks. The temperature corresponding to the peak maxima is reported as a function of T_c in *Figure 13* for pure Nylon, Ny/EPM 80/20, Ny/EPM-g-SA 80/20, and Ny/EPM/EPM-g-SA 80/10/10 blends. From the analysis of these curves it emerges that the addition of rubber to Ny 6 does not influence the thermal behaviour of the Ny and that the peak at higher temperature is present only for T_c lower than 466 K. The equilibrium melting temperature T_m of the α form of Ny 6 is reported in *Table 3* as a function of blend composition.

The values of T_m have been obtained by using Hoffman's equation[15]:

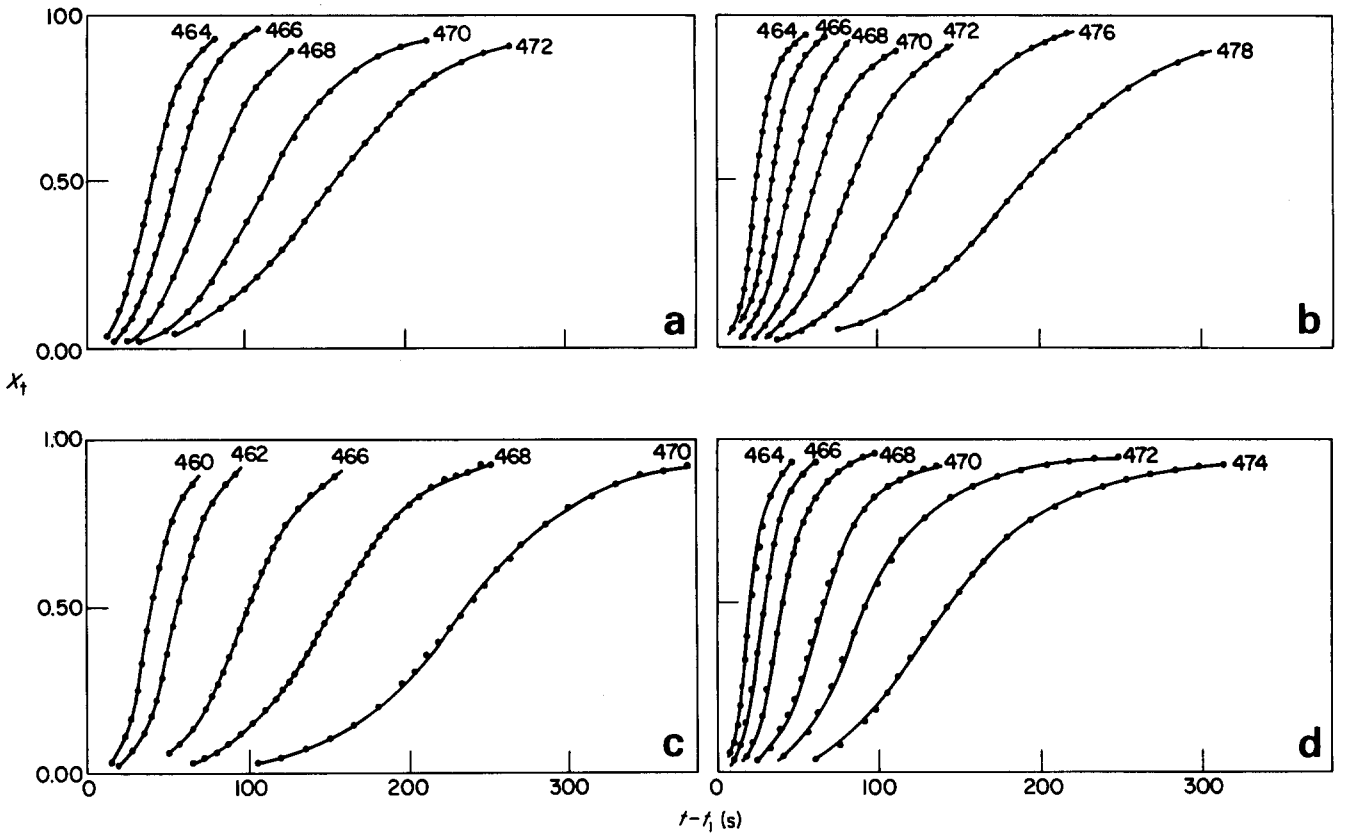

Figure 16 Typical isothermals of crystallization at different T_c. (a) Ny 100%; (b) Ny/EPM 80/20; (c) Ny/EPM-g-SA 80/20; (d) Ny/EPM/EPM-g-SA 80/10/10

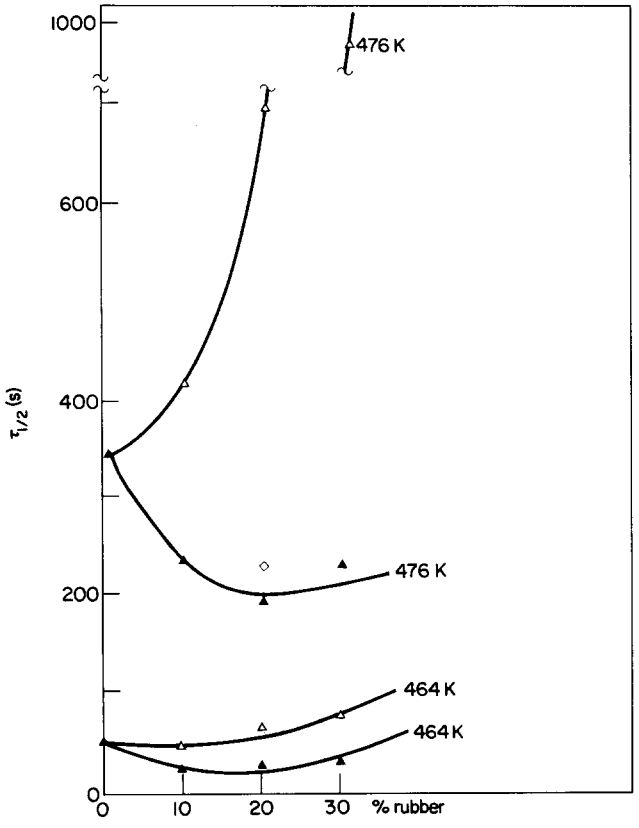

Figure 17 Half-time of crystallization against rubber content for two T_c as indicated on the Figure. (▲) Ny/EPM; (△) Ny/EPM-g-SA; (◇) Ny/EPM/EPM-g-SA 80/10/10

$$T_m' = T_m\left(1-\frac{1}{\gamma}\right)+\frac{T_c}{\gamma} \qquad (2)$$

where γ is a morphological factor. As shown in *Table 3*, T_m is almost independent of composition and chemical structure of the rubber; a small increase is observed only in the case of 90/10 Ny/EPM-g-SA blend.

Glass transition temperatures. The d.s.c. thermograms of the starting polymers are reported in *Figure 14*. For the pure Ny, in the range of temperature studied, it is possible to note two high order transitions: at 42°C and at 0°C. The first transition corresponds, according to literature data[16], to the glass transition temperature, whereas the second is likely to be related to the presence of water in the sample.

The thermograms of EPM and EPM-g-SA are similar to each other (see *Figure 14*). The T_g is at about −50°C whereas at 43°C an endothermic peak due to the melting of ethylene block is observed. Typical thermograms for the blends are reported in *Figure 15*. From this Figure it is possible to note that the value of T_g of the rubber phase is −50°C. Unfortunately the T_g of the Ny phase is covered by the melting peak and cannot be detected.

Moreover it seems that the T_g of the two phases in the blends do not undergo substantial variations. This result together with the observation that the T_m is almost independent of rubber content leads to conclude that the Ny, EPM and EPM-g-SA are incompatible in the melt[17].

Kinetics of isothermal crystallization

Typical crystallization isotherms obtained by plotting X_t (weight fraction of crystallinity at times (t) against time

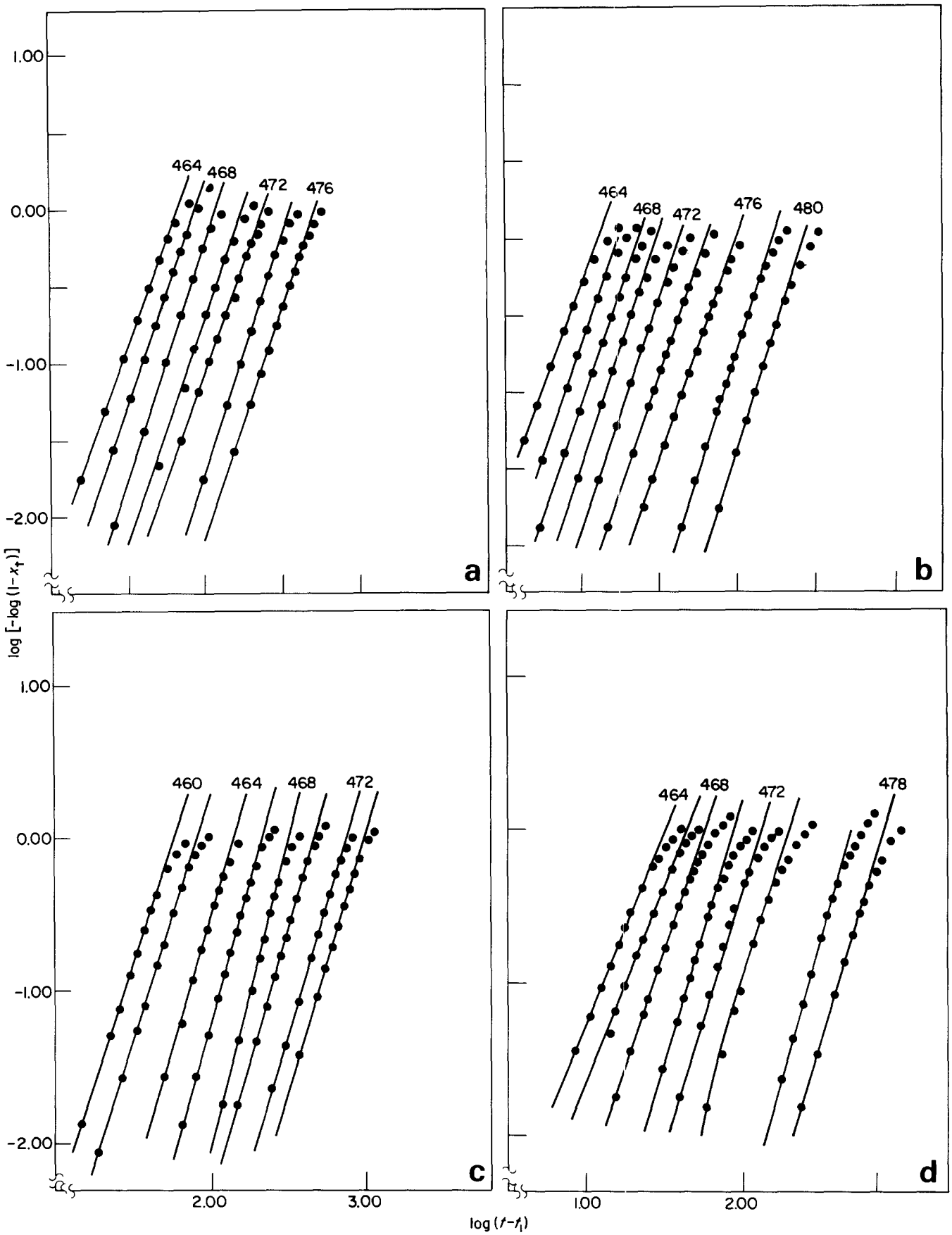

Figure 18 Avrami's plots for the crystallization of Ny and Ny/EPM 80/20, Ny/EPM-g-SA 80/20 and Ny/EPM/EPM-g-SA 80/10/10 blends (a) Ny 100%; (b) Ny/EPM 80/20; (c) Ny/EPM-g-SA 80/20; (d) Ny/EPM/EPM-g-SA 80/10/10

(t) are reported in *Figure 16* for the pure Ny and for the Ny/EPM 80/20, Ny/EPM-g-SA 80/20 and Ny/EPM/EPM-g-SA 80/10/10 blends. From these curves the half time of crystallization, $\tau_{1/2}$, defined as the time taken for half of the crystallinty to develop, is obtained. Plots of $\tau_{1/2}$ against rubber content for two different

Table 4 K_n (s^{-n}) values as function of composition and T_c for nylon 6 and its blends with EPM and EPM-g-SA

Sample		T_c = 460 K	T_c = 462 K	T_c = 464 K	T_c = 466 K	T_c = 468 K	T_c = 470 K	T_c = 472 K	T_c = 474 K	T_c = 476 K	T_c = 478 K	T_c = 480 K
Ny	100%			1.6×10^{-5}	5.1×10^{-6}	8.4×10^{-7}	4.4×10^{-7}	4.8×10^{-7}	2.8×10^{-8}	1.7×10^{-8}		
Ny/EPM	90/10			3.8×10^{-4}	3.8×10^{-5}	6.2×10^{-6}	4.5×10^{-7}	9.0×10^{-8}	7.9×10^{-8}	1.8×10^{-8}	9.4×10^{-9}	1.8×10^{-8}
Ny/EPM	80/20			9.5×10^{-5}	1.8×10^{-5}	4.5×10^{-6}	2.9×10^{-6}	7.20×10^{-7}	2.2×10^{-7}	9.6×10^{-8}	1.7×10^{-9}	3.5×10^{-10}
Ny/EPM	70/30			7.1×10^{-5}	1.2×10^{-5}	1.3×10^{-6}	4.0×10^{-8}	3.8×10^{-8}	3.2×10^{-8}	3.2×10^{-8}	1.0×10^{-9}	3.2×10^{-9}
Ny/EPM-g-SA	90/10	2.5×10^{-4}	1.6×10^{-5}	4.4×10^{-6}	4.1×10^{-7}	2.8×10^{-8}	2.1×10^{-8}	2.2×10^{-10}	2.2×10^{-10}	7.7×10^{-11}		
Ny/EPM-g-SA	80/20	5.2×10^{-6}	1.2×10^{-6}	1.7×10^{-6}	1.1×10^{-7}	1.3×10^{-9}	2.0×10^{-9}	5.9×10^{-10}	4.0×10^{-10}	1.11×10^{-9}		
Ny/EPM-g-SA	70/30	4.0×10^{-5}	2.8×10^{-6}	2.7×10^{-7}	4.0×10^{-8}	9.2×10^{-9}	2.5×10^{-9}	3.7×10^{-10}	3.6×10^{-11}	9.6×10^{-11}		
Ny/EPM/EPM-g-SA	80/15/5			2.0×10^{-4}	2.5×10^{-5}	1.7×10^{-6}	7.5×10^{-7}	1.6×10^{-7}	4.5×10^{-9}	1.9×10^{-8}	1.9×10^{-9}	9.8×10^{-11}
Ny/EPM/EPM-g-SA	80/10/10			4.6×10^{-4}	1.5×10^{-4}	10×10^{-5}	6.9×10^{-7}	3.4×10^{-7}	5.2×10^{-8}	1.5×10^{-8}	2.4×10^{-10}	5.11×10^{-10}

crystallization temperatures are reported in *Figure 17*. From these curves it emerges that the $\tau_{1/2}$ of the Ny phase depends on the type of copolymer added. In fact for the Ny/EPM-g-SA blends the half time of crystallization increases with the increase of the rubber content, whereas in the case of Ny/EPM blend a drop in $\tau_{1/2}$ for lower EPM content, followed by an almost constant trend, is observed. In the case of ternary blends, for the same T_c, the values of $\tau_{1/2}$ are very close to those of the Ny/EPM 80/20 blends.

Taking into account the morphological observation that the EPM-g-SA acts as a nucleating agent, then the drastic reduction of the overll rate of crystallization in Ny/EPM-g-SA blends is likely to be related to the increase of the viscosity that the system undergoes (as confirmed by torque measurements)[18].

In principle a nucleating effect causes an increase of the overall crystallization rate, whereas an increase of viscosity decreases the spherulite growth rate G. The equation that links the spherulitic growth rate, G, with the overall kinetic rate constant of crystallization (K_n) in the case of three-dimensional crystallization and sporadic nucleation is the following[19]:

$$K_n = \frac{4\pi\rho_c}{3\rho_a(1-\lambda_\infty)} \times G^3\bar{N} \tag{3}$$

where ρ_a and ρ_c are the density of the amorphous and crystalline phase respectively, $(1-\lambda_\infty)$ is the overall crystallinity at the time $t=\infty$ and $\bar{N}$ the nucleation density.

The fact that the addition of EPM-g-SA to Ny causes a decrease in the overall crystallization rate and hence in K_n values seems to indicate on the basis of equation (3), that the effect due to the increase of melt viscosity prevails, under the experimental conditions used, over the nucleating effect. In the case of EPM containing blends the increase observed in the crystallization rate may be attributed to a slight nucleating effect and/or to a slight decrease of the viscosity in the melt state.

The overall kinetics of crystallization of nylon and its blends with rubbers follows the Avrami equation[19]:

$$\log[-\log(1-X_t)] = \frac{1}{2.3}\log K_n + n\log t \tag{4}$$

where n is the Avrami index. In fact plots of $\log[-\log(1-X_t)]$ against $\log t$ are linear, no change in the slope being observed until long times of conversion (see *Figure 18*). The values of K_n and n determined by the intercepts and slopes respectively of these straight lines are reported in *Tables 4* and *5*.

The n values vary between 2.4 and 4.0 almost irrespective of T_c, type of rubber and composition. The fact that the Avrami index is almost independent of the composition and type of copolymer indicates that the rubber does not influence the mechanism of nucleation and growth of the Ny crystals.

Temperature dependence of the overall crystallization kinetic rate constant

Assuming that the process of crystal growth during the primary crystallization is controlled by a surface coherent two dimensional secondary nucleation process, then in accordance with the kinetic theory of polymer cyrstalli-

Table 5 Avrami index for nylon 6 and its blends with EPM and EPM-g-SA

Sample		T_c = 460 K	T_c = 462 K	T_c = 464 K	T_c = 466 K	T_c = 468 K	T_c = 470 K	T_c = 472 K	T_c = 474 K	T_c = 476 K	T_c = 478 K	T_c 480 K
Ny	100%			2.8	2.9	3.1	3.0	2.8	3.1	3.0		
Ny/EPM	90/10			2.6	2.7	2.9	3.3	3.4	3.2	3.2	3.1	2.8
Ny/EPM	80/20			2.8	3.0	3.1	3.0	3.0	3.1	3.1	3.4	3.4
Ny/EPM	70/30			2.7	2.9	3.3	3.3	3.5	3.3	3.1	3.4	3.0
Ky/EPM-g-SA	90/10	2.6	3.1	3.2	3.5	3.8	3.6	3.5	3.9	3.8		
Ny/EPM-g-SA	80/20	3.2	3.3	3.1	3.4	4.0	3.6	3.6	3.4	3.1		
Ky/EPM-g-SA	70/30	2.7	3.1	3.4	3.5	3.5	3.5	3.6	3.7	3.3		
Ny/EPM/EPM-g-SA	80/15/5			2.5	2.9	3.3	3.2	3.3	3.7	3.2	3.3	3.5
Ny/EPM/EPM-g-SA	80/10/10			2.4	2.5	3.0	3.3	3.2	3.3	3.3	3.7	3.3

Table 6 Free energy of formation of a nucleus of critical size $\Delta\phi$ (erg) x 10^{13}

Sample		T_c = 460 K	T_c = 462 K	T_c = 464 K	T_c = 466 K	T_c = 468 K	T_c = 470 K	T_c = 472 K	T_c = 474 K	T_c = 476 K	T_c = 478 K	T_c = 480 K
Ny	100%			4.7	4.9	5.2	5.5	5.8	6.2	6.6		
Ny/EPM	90/10			4.6	4.9	5.1	5.4	5.7	6.0	6.4	6.9	7.4
Ny/EPM	80/20			4.4	4.7	4.9	5.2	5.5	6.8	6.2	6.6	7.2
Ny/EPM	70/30			4.3	4.6	4.8	5.0	5.3	5.7	6.1	6.5	7.0
Ny/EPM-g-SA	90/10	5.7	5.9	6.2	6.4	6.8	7.1	7.5	7.9	8.3		
Ny/EPM-g-SA	80/20	5.3	5.6	5.8	6.1	6.4	6.7	7.1	7.5	8.0		
Ny/EPM-g-SA	70/30	5.3	5.6	5.8	6.1	6.5	6.8	7.2	7.7	8.2		
Ny/EPM/EPM-g-SA	80/15/5			4.9	5.2	5.4	5.7	6.0	6.4	6.8	7.2	7.8
Ny/EPM/EPM-g-SA	80/10/10			4.7	4.9	5.2	5.5	5.8	6.1	6.6	7.0	7.6

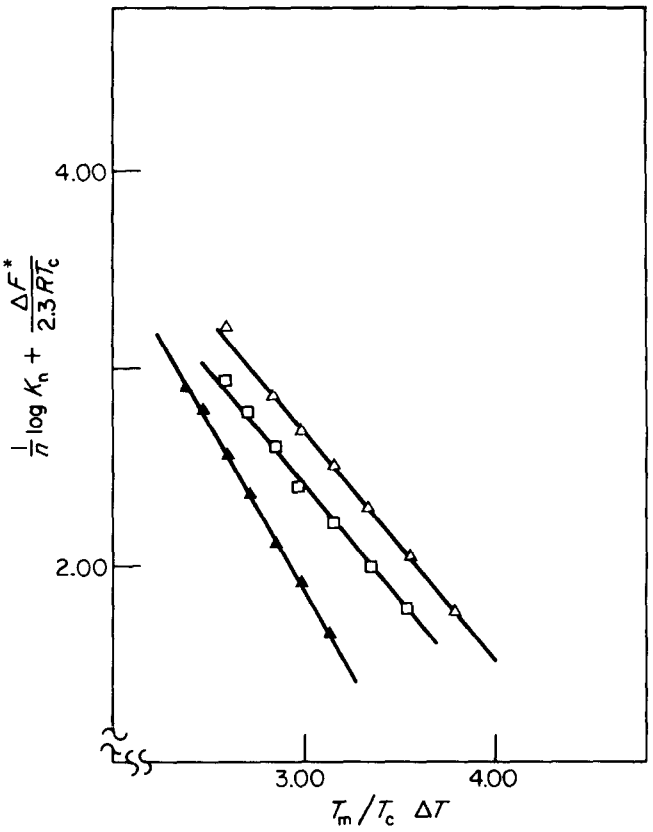

Figure 19 Plots of $\frac{1}{n}\log K_n + \frac{\Delta F^*}{2.3RT_c}$ *versus* $T_m/T_c\Delta T$ for the (□) Ny 100%, (▲) Ny/EPM 80/20 and (△) Ny/EPM-g-SA 80/20

zation, the temperature dependence of the overall kinetic rate constant may be expressed by the relation[19,20]:

$$\frac{1}{n}\log K_n + \frac{\Delta F^*}{2.3RT_c} = A_n - \frac{\Delta\Phi^*}{2.3KT_c} \qquad (5)$$

where ΔF^* is the activation energy for the transport of the molecules from the liquid to the solid interface; usually taken from the WLF time–temperature superposition principle[21] as:

$$\Delta F^* = \frac{c_1 T_c}{c_2 + T_c - T_g} = \frac{4120\,T_c}{51.6 + T_c - T_g}$$

A_n can be considered as a constant if the density of primary nucleation at T_c is not dependent on time; $\Delta\phi^*$ is the free energy of formation of a nucleus of critical size expressed as:

$$\Delta\phi^* = \frac{4b_0\sigma\sigma_e T_m}{\Delta H_f(T_m - T_c)} \qquad (6)$$

where b_0 is the distance between two adjacent fold planes, σ and σ_e are the free energy of formation of the lateral and folding surface of lamellar crystals.

Equation (5) fits quite well the experimental data for all samples investigated. In fact plots of $\frac{1}{n}\log K_n \frac{+\Delta F^*}{2.3\,RT_c}$ *versus* $T_m/(T_c\Delta T)$ give always straight lines (see *Figure 19*). From the slope of such lines the values of $\Delta\phi^*$ and σ_e are obtained setting $\sigma = 0.1\Delta H_f b_0$[19] and $b_0 = 4.25 \times 10^{-10}$ m[10]. The values of $\Delta\phi^*$ and σ_e are reported in *Tables 6* and *7*.

Table 7

Sample		σ_e (erg/cm^2)
Ny	100%	54
Ny/EPM	90/10	55
Ny/EPM	80/20	51
Ny/EPM	70/30	50
Ny/EPM-g-SA	90/10	77
Ny/EPM-g-SA	80/20	70
Ky/EPM-g-SA	70/30	67
Ny/EPM/EPM-g-SA	80/5/15	59
Ny/EPM/EPM-g-SA	80/10/10	54

It can be observed that σ_e and $\Delta\phi^*$ of Ny 6/EPM-g-SA blends are larger than those of plain nylon 6 whereas an opposite trend is found in the case of nylon 6/EPM blends. Moreover both σ_e and $\Delta\phi^*$ for a given type of blend seem to decrease with the increase of rubber content.

ACKNOWLEDGEMENT

Partial financial support of this work by the Progetto Finalizzato 'Chimica Fine e Secondaria' of the C.N.R. is gratefully acknowledged. The authors wish to thank Mr L. Amelino who carried out the measurements of the glass transition temperatures.

REFERENCES

1 Cimmino, S., D'Orazio, L., Greco, R., Maglio, G., Malinconico, M., Mancarella, C., Martuscelli, E., Palumbo, R. and Ragosta, G. *Polym. Eng. Sci.* in press
2 Cimmino, S., D'Orazio, L., Greco, R., Maglio, G., Malinconico, M., Mancarella, C., Martuscelli, E., Musto, P., Palumto, R. and Ragosta, G. *Polym. Eng. Sci.* in press
3 Martuscelli, E., Riva, F., Sellitti, C. and Silvestre, C. 'Crystallization, Morphology, Structure and Thermal Behaviour of Nylon 6/Rubber Blends'. Presented at International Symposium on Phase Relationships and Properties of Multicomponent Polymer Systems, Anacapri, May 30–June 3, 1983
4 Kyotani, M. and Mitsuhashi, S. *J. Polym. Sci. A-2* 1972, **10**, 1497
5 Dole, M. and Wunderlich, B. *B. Makromol. Chem.* 1959, **34**, 29
6 Holmes, R., Bunn, C. W. and Smith, D. J. *J. Polym. Sci.* 1955, **17**, 159
7 Hosemann, R. and Bagchi, S. N. 'Direct Analysis of Diffraction by Matter', North Holland, Amsterdam, 1962
8 Martuscelli, E., Silvestre, C. and Abate, G. C. *Polymer* 1982, **23**, 229
9 Martuscelli, E., Silvestre, C. and Bianchi, L. *Polymer* 1983, **24**, 1458
10 Privalko, V. P., Tawai, T. and Lipatov, Yu. S. *Polym. J.* 1979, **11**, 669
11 Illers, K. H. and Huberkorn, H. *Makromol. Chem.* 1971, **142**, 31
12 Gurato, G., Fichera, A., Grandi, F. Z., Zanetti, R. and Canal, P. *Makromol. Chem.* 1974, **175**, 953
13 Valenti, B., Greppi, G., Tealdi, A. and Ciferri, A. *J. Phys. Chem.* 1975, **77**, 389
14 Arakawa, T., Nagatoshi, F. and Arai, N. *J. Polym. Sci. A-2* 1969, **7**, 1461
15 Hoffmann, J. D. *SPE Trans.* 1954, **4**, 315
16 Kohan, M. I. 'Nylon Plastics', John Wiley and Sons, New York
17 Paul, D. R. 'Polymer Blends' (Eds. D. R. Paul and S. Newman), Academic Press, New York, 1978
18 Greco, R. private communication
19 Mandelkern, L. 'Crystallization of Polymer', McGraw-Hill, N.Y., 1964
20 Turnbull, D. and Fisher, J. C. *J. Chem. Phys.* 1949, **17**, 71
21 Williams, M. L., Landel, R. F. and Ferry, J. D. *J. Am. Chem. Soc.* 1955, **77**, 3701